Inorganic Chemistry
Cite This: Inorg. Chem. XXXX, XXX, XXX–XXX
Article
pubs.acs.org/IC

Flexible Metal–Organic Frameworks for Light-Switchable CO_2 Sorption Using an Auxiliary Ligand Strategy

Debobroto Sensharma, Nianyong Zhu, Swetanshu Tandon, Sebastien Vaesen, Graeme W. Watson, and Wolfgang Schmitt*

School of Chemistry & AMBER Centre, The University of Dublin, Trinity College Dublin, Dublin D2, Ireland

Supporting Information

ABSTRACT: We report the synthesis and characterization of two photoactive metal–organic frameworks (MOFs), **TCM-14** and **TCM-15**. The compounds were synthesized by incorporating 4,4′-azopyridine auxiliary ligands into **pto**-type scaffolds that are composed of dinuclear copper(II) "paddle-wheel"-based secondary building units and flexible, acetylene-extended, tritopic benzoate linkers. Room temperature CO_2 sorption of the MOFs was studied, and UV-light irradiation is shown to result in reduced CO_2 adsorption under static conditions. **TCM-15** reveals a dynamic response leading to an instant desorption of up to 20% of CO_2 upon incidence of UV light because of the occurrence of nonperiodic structural changes. Physicochemical and computational density functional theory studies were carried out to gain insight into the mechanism of the interaction of light with the frameworks.

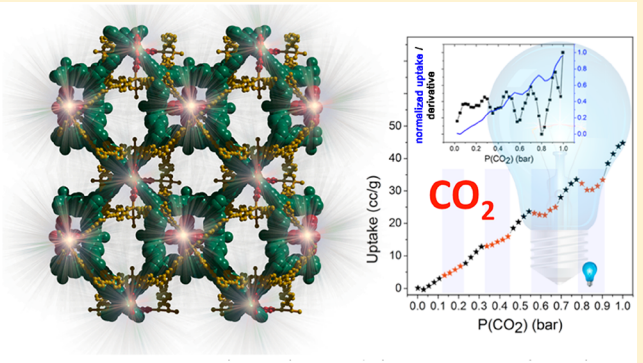

INTRODUCTION

Structurally tailored and synthetically functionalized metal–organic frameworks (MOFs) have emerged as materials with promising applications in the separation and storage of gases because of their unprecedented surface areas, selectivities, storage capacities, and, importantly, facile reversible recovery of the adsorbates.[1−4] In order to design breathable or stimuli-responsive materials that facilitate the uptake and release of guests on demand, unconventional energy inputs are the subject of intensive scientific investigation.[5] Because MOFs offer a highly modular and tunable platform, a number of pathways for synthetic modification are being explored. New synthetic routes to the design of stimuli-responsive MOFs, incorporating the desired functionalities, are therefore key to improving the applicability of these materials. One sustainable, cheap, and abundant source of energy is light; it is ubiquitous in the form of solar radiation and its incidence upon a system can easily be controlled at low cost. Thus, flexible photoactive MOFs (or related covalent–organic frameworks, COFs) are intriguing new classes of materials to elucidate the fundamental effects that govern the influence of light-induced structural changes on the uptake/release of adsorbates.[6,7]

A large number of MOFs that are stabilized by polytopic carboxylates contain metal sites capped with labile neutral ligands (often solvent) that can easily be removed or replaced to yield unsaturated metal centers (UMCs).[8] For some specific framework topologies, for instance, **pto** (Pt_3O_4-type net) or **pts** (PtS-type net), assuming the use of a single polytopic carboxylate ligand, such sites are located diametrically across structural voids from each other. This allows the conception of suitable bridging secondary linkers introduced across the void space to functionalize the material, as utilized by Kaskel and co-workers, as well as previous work in our group. Such secondary (or auxiliary) linkers may be used to introduce functional groups suitable for various applications into the architecture of specific MOFs.[9−12]

Responsive MOFs that show light-induced changes in porosity are of increasing research interest as alternatives to conventional pressure-swing and temperature-swing techniques.[13] These MOFs are primarily of three types—those containing photosensitive guest molecules, nanoparticles, or surface coatings,[14−16] those with photoisomerizable pendant groups built into their ligands,[17−21] and those with photoresponsive groups built integrally into the ligand backbone of the MOF[22−25]—in addition to more intricate methods.[26,27] With the exception of the third technique, these methods require partial restriction or blocking of the MOF pore, resulting in reduced adsorbate uptake. Further, building these photoresponsive groups into the backbone of the framework allows real-time responses to light, allowing for high-speed release of the adsorbate gas, whereas with guests or pendant groups that isomerize in response to light, factors such as steric hindrance within each cavity lead to relatively slow responses. Suppressed bending or pedal-like motion of the ligands has been shown to produce significant dynamic changes in uptake

Received: March 18, 2019

DOI: 10.1021/acs.inorgchem.9b00768
Inorg. Chem. XXXX, XXX, XXX–XXX

despite the modest magnitude of the induced structural change.[25,28] Ligands that display photoresponsive behavior when incorporated in MOFs are mainly based on azobenzene and dithienylethene moieties, which are well-known species used in molecular switches.[29−31]

In this study we describe the use of 4,4′,4″-benzene-1,3,5-triyltris(ethyne-2,1-diyl)tribenzoic acid (H_3bteb) ligands in combination with paddle-wheel SBUs in order to obtain **pto** nets that are further modified using auxiliary linkers (Figure 1).

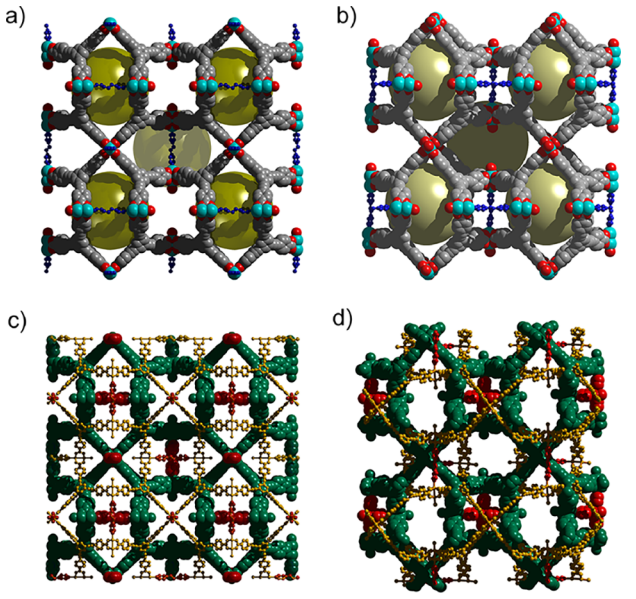

Figure 1. Framework structures of (a) **TCM-14** and (b) **TCM- 15**, respectively (azopyridine moieties are highlighted in blue; Cu atoms are teal, O atoms red, and C atoms gray, while H atoms are omitted; void volumes are indicated as yellow spheres). (c and d) Dual-interpenetrated structures of **TCM-14** and **TCM-15**, respectively [azopyridine moieties are highlighted in red; respective interwoven frameworks are shown in space-filling (green) and ball-and-stick (orange) modes].

H_3bteb is an extended tritopic ligand that is significantly flexible in two respects, relative to more common, shorter tricarboxylate ligands such as 4,4′,4″-benzene-1,3,5-triyltris-(benzoic acid) (H_3btb). First, the acetylene moieties lengthen each arm, resulting in mechanical flexibility manifested as ligand bowing, which can be seen in the crystal structures of MOFs based on H_3bteb. Second, the acetylene moieties remove Ar_H−Ar_H repulsion, which restricts rotation of the peripheral benzoate moieties relative to the central phenyl ring. Therefore, bteb^{3-} can form **pto**, **tbo** (twisted boracite-type net), and other networks, and the use of auxiliary ligands can direct the formation of phase-pure **pto** MOFs.[32−34]

Here, we take advantage of the tunability of the **pto** arrangement and incorporate functionalities into the MOF pore. In compounds **TCM-14** and **TCM-15**, the H_3bteb ligand is combined with {Cu_2} paddle-wheel SBUs, and the **pto** framework formed is decorated with auxiliary 4,4′-azopyridine (azpy) ligands chosen for their photoresponsive behavior upon irradiation using UV light (Scheme 1). **TCM-14** and **TCM-15** were characterized by single-crystal X-ray diffraction (SCXRD) and physicochemical techniques, and their photoresponse is evaluated in the context of gas sorption. Some early studies concluded that the photoresponse could not be shown if the photoresponsive ligands were integral to the framework

Scheme 1. Applied Synthetic Approach for the Targeted Synthesis of Functionalized pto-Based MOFs[a]

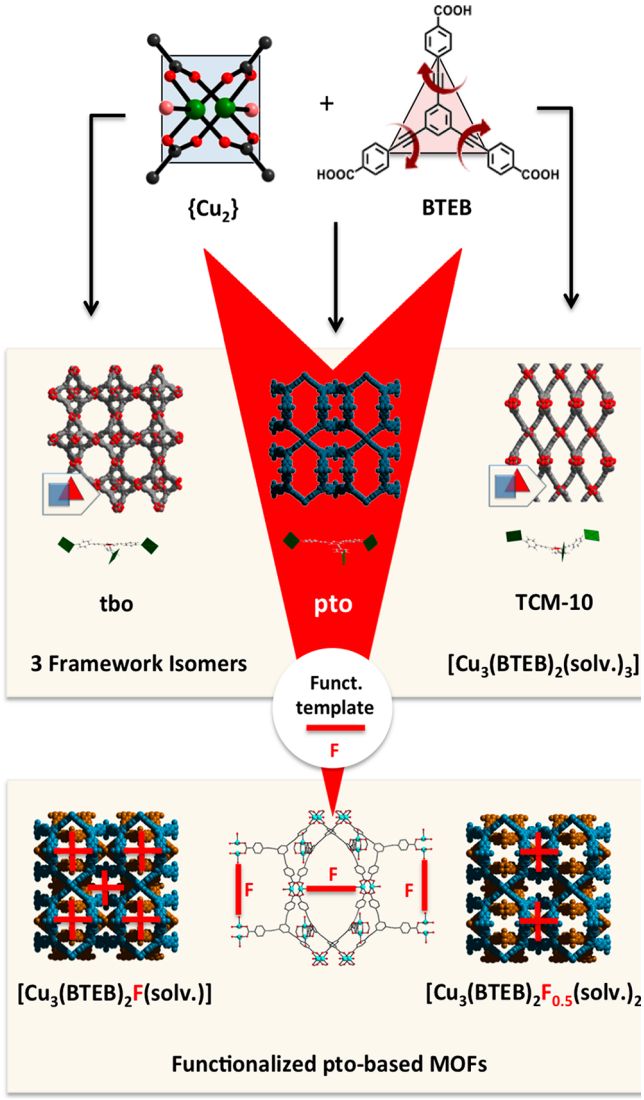

[a]The functionalizing secondary ligands (F) promote the formation of **pto** topology over competing possible framework isomers. The stoichiometric quantity of F determines the degree of functionalization and gives rise to the formation of MOFs with two constitutional compositions, [Cu_3(bteb)$_2$F(solv)] and [Cu_3(bteb)$_2F_{0.5}$(solv)$_2$]. Solv. = coordinating solvent molecules, here DMF or H_2O.

backbone, a conclusion revised after sufficiently flexible frameworks were tested. **TCM-14** and **TCM-15** are the first based on azpy, as well as the first based on a mixed-ligand approach to show responsive sorption behavior enabled by the combination of a photoresponsive ligand and an unresponsive flexible ligand.

EXPERIMENTAL SECTION

Synthesis of 4,4′,4″-(Benzene-1,3,5-triyltris(ethyne-2,1-diyl)tribenzoic Acid (H_3bteb). H_3bteb was synthesized according to a modified literature procedure.[35]

Synthesis of [Cu_3(bteb)$_2$(azpy)(H_2O)] (TCM-14). A total of 0.0254 g of H_3bteb (0.05 mmol) and 0.0177 g of $Cu(NO_3)_2{\cdot}3H_2O$ were added to 1 mL of DMF in a glass vial and sonicated for 10 min. A total of 0.0033 g of azpy (0.0018 mmol) was added to the reaction mixture. The vial was sealed and heated at 85 °C for 24 h. Green crystals of **TCM-14** were obtained. The crystals were washed with

DOI: 10.1021/acs.inorgchem.9b00768
Inorg. Chem. XXXX, XXX, XXX−XXX

and stored under DMF. Yield: 60%. Elem. anal. Calcd for $C_{76}H_{40}Cu_3O_{13}N_4$ (including eight constitutional H_2O molecules): C, 58.82; H, 3.64; N, 3.61. Found: C, 58.57; H, 3.14; N, 4.14.

Synthesis of $[Cu_3(bteb)_2(azpy)_{0.5}(H_2O)_2]$ (TCM-15). A total of 0.0254 g of H_3bteb (0.05 mmol) and 0.0177 g of $Cu(NO_3)_2{\cdot}3H_2O$ were added to 1 mL of DMF in a glass vial and sonicated for 10 min. A total of 0.0011 g of azpy (0.0006 mmol) was added to the reaction mixture. The vial was sealed and heated at 85 °C for 8 h. Green crystals of **TCM-15** were obtained as a minor product. The crystals were separated by hand and washed with and stored under DMF. Yield: 10%. Elem. anal. Calcd for $C_{142}H_{76}Cu_6N_4O_{28}$ (including six constitutional H_2O molecules): C, 61.45; H, 3.20; N, 2.02. Found: C, 61.59; H, 2.56; N, 1.93.

RESULTS AND DISCUSSION

SCXRD studies carried out on **TCM14** and **TCM-15** show the adoption of doubly interwoven structures based on the **pto** net. The frameworks are constituted by dinuclear Cu^{2+} paddle-wheel SBUs bound by *syn,syn*-bidentate carboxylate groups from the fully deprotonated $bteb^{3-}$ ligand. Each ligand is connected to three $\{Cu_2\}$ paddle-wheel units, and each $\{Cu_2\}$ paddle-wheel is connected to four $bteb^{3-}$ ligands to form a 4,3-connected net, in which torsions of ca. 33° between the central and peripheral phenyl rings stabilize the **pto** arrangement.

The **pto** networks in both MOFs have $Cu^{2+}{-}Cu^{2+}$ axes aligned in three perpendicular directions, which are coincident to the three crystallographic axes (the distance between opposite SBUs is ca. 13.4 Å). Both can be considered substituted versions of the archetype **pto** framework reported in **TCM-4** ($[Cu_3(bteb)_2(H_2O)_3]$) and modified in **TCM-5** ($[Cu_3(bteb)_2(bpy)_{0.5}(H_2O)_2]$).[10] The azpy linker (length: ca. 9.1 Å), despite its slight nonlinearity, is a highly suitable auxiliary ligand for incorporation into the **TCM-4** structure. In contrast to polytopic carboxylates, the incorporation of ditopic N-donor bridges allows rotational freedom for the auxiliary ligand about the terminal N-terminal N axis, provided there are suitable sterics. Mismatches in length are compensated for by the highly extended $bteb^{3-}$ ligand, which shows a great capacity for bowing, and some stabilization is afforded by aromatic interactions between the two interwoven frameworks.

TCM-14 crystallizes in the space group *P*42/*nmc*; deviation from the cubic symmetry seen in **TCM-4** results in adoption of the tetragonal crystal system. Along the crystallographic *a* and *b* axes, alternate inter-SBU spaces are bridged by azpy ligands, leaving H_2O molecules coordinated to half of the Cu^{2+} centers. However, along the crystallographic *c* direction, all SBUs are bridged. This results in an overall molecular formula of $[Cu_3(bteb)_2(azpy)(H_2O)]$, with dual interpenetration.

From this perspective, **TCM-15** offers a more desirable compromise between the porosity and incorporation of the switching functionality via the azpy ligand. The compound crystallizes in the triclinic crystal system (space group $P\bar{1}$). As in **TCM-14**, the structure is based on dinuclear Cu^{2+} paddle-wheel SBUs (the $Cu^{2+}{-}Cu^{2+}$ distance is ca. 2.64 Å) and $bteb^{3-}$ ligands. The presence of fewer azpy bridging ligands results in permanent channels that are characterized by a cross-sectional diameter of 8.8 Å at their narrowest, extending in the direction of the crystallographic *c* axis. Alternate inter-SBU spaces along the crystallographic *a* and *b* axes are bridged by azpy ligands, while SBUs along the *c* direction retain axially coordinated H_2O ligands. This arrangement results in greater channel availability because of a lower number of auxiliary ligands and a larger number of potential UMCs upon activation, which are known to interact with CO_2 adsorbate molecules. Thus, in contrast to **TCM-14**, in **TCM-15**, the $\{Cu_2\}$ units are not linked into a continuous 1D arrangement by azpy ligands in any direction. Therefore, the composition of **TCM-15** is $[Cu_3(bteb)_2(azpy)_{0.5}(H_2O)_2]$, with dual interpenetration.

Topological analysis reveals that **TCM-14** consists of two identical, interpenetrating 3,5,6-connected 3-nodal nets. The overall point symbol for each of these nets is $\{5^{12}{\cdot}8^3\}\{5^2{\cdot}8\}_4\{5^6{\cdot}8^4\}_2$. Similarly, **TCM-15** consists of two identical, interpenetrating 3,4,5-connected 3-nodal nets, with point symbol $\{5{\cdot}8^2\}_4\{5^6{\cdot}8^4\}_2\{8^6\}$.[36] The presence of 6-connected nodes in **TCM-14** and 4-connected nodes in **TCM15** is consistent with the observed degrees of azpy incorporation (Figure 2). These two nets may be termed intermediates between the "empty" **pto** net, and the "fully bridged" **ith-d** net, and can be considered to be derived from the **pto** archetype by the incorporation of azpy ligands.[37,38] The void volumes in **TCM-14** and **TCM-15** correspond well with the thermogravimetric analysis (TGA) under N_2, and framework stability up to 280 °C was observed. Fourier transform infrared (FTIR) spectroscopy and powder X-ray diffraction (PXRD) studies further corroborate the structures of **TCM-14** and **TCM-15** (see the Supporting Information, SI).

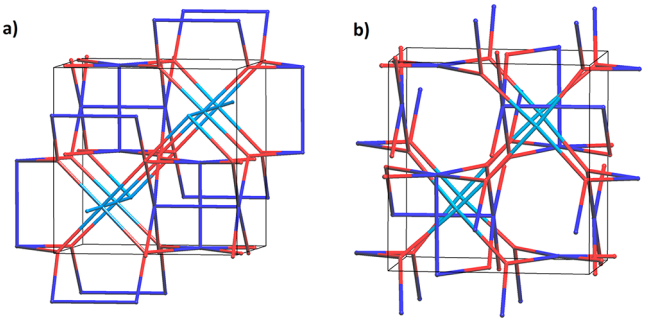

Figure 2. Topological representations of the unit cells of doubly interwoven (a) **TCM-14** and (b) **TCM-15**. The 3-connected nodes are shown in red (corresponding to $bteb^{3-}$), and the 4-, 5-, and 6-connected nodes are in shades of blue (corresponding to variously coordinated $\{Cu_2\}$ units).

Having confirmed the thermal stability and possible porosity of the compounds, both MOFs were subjected to gas sorption analysis. Activation directly from DMF and activation using supercritical CO_2 resulted in nonporous samples of **TCM-14** and **TCM-15** because of the fragility of their low-density paddle-wheel-based structures.[38] Activation performed under secondary vacuum at 120 °C following solvent exchange with CH_2Cl_2 for a short duration was carried out, with the additional precaution of a valve to prevent exposure to ambient conditions after activation (see the SI). This method reliably produced samples of **TCM-14** and **TCM-15** that physisorb CO_2. The porosity to N_2 at 77 K was not significant even after such activation (see the SI). We attribute this effect to the larger kinetic diameter of N_2 and weaker interactions of N_2 with the material, as well as a degree of amorphization and collapse of the framework structure. CO_2 adsorption experiments were carried out on both samples at 293 K, and the measurement temperature was maintained carefully using a recirculating water bath. While framework collapse had a clear effect on the overall magnitude of the CO_2 uptake, the measurements carried out in the dark confirmed a substantial degree of CO_2 physisorption by the materials despite their fragility.

DOI: 10.1021/acs.inorgchem.9b00768
Inorg. Chem. XXXX, XXX, XXX−XXX

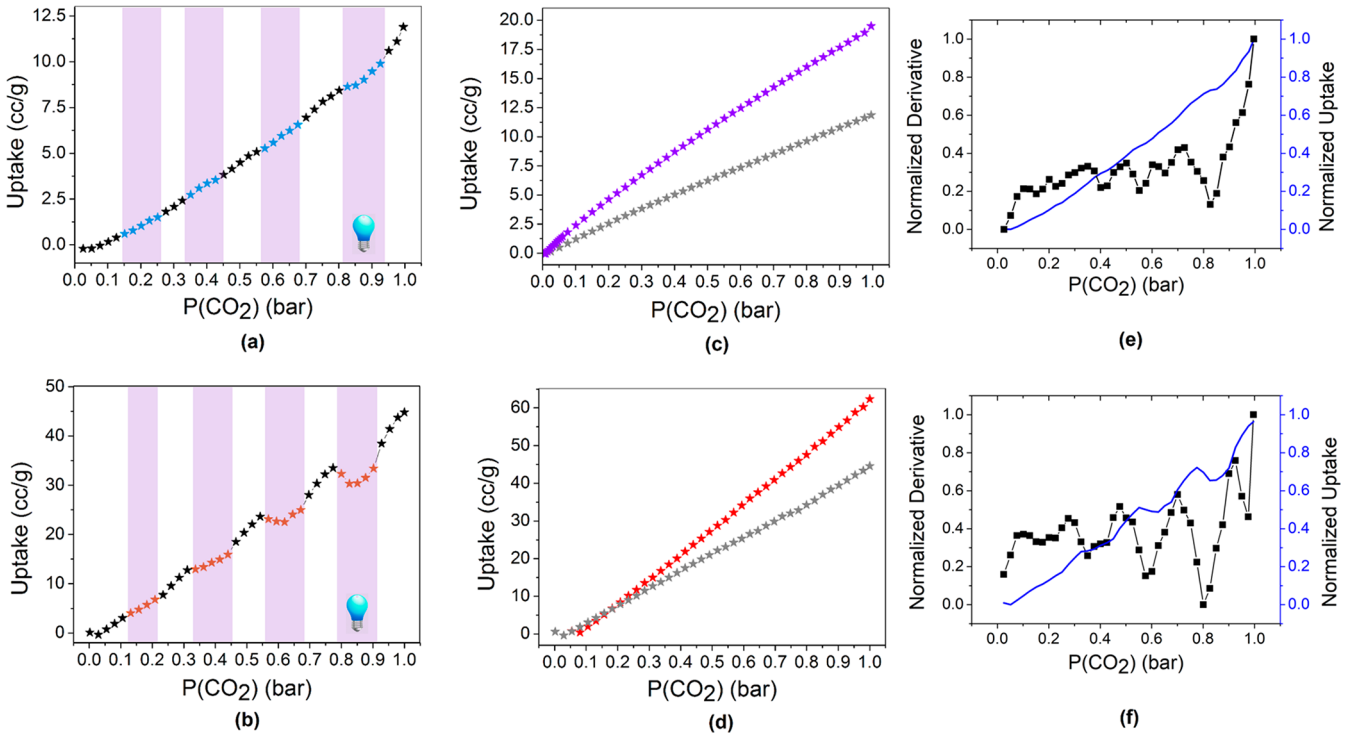

Figure 3. CO_2 adsorption isotherms (293 K) for **TCM-14** under (a) dynamic irradiation (black, in the dark; light blue, under UV-light irradiation) and (c) static irradiation (purple, in the dark; gray, under UV-light irradiation), and (e) the derivative of the isotherm under dynamic conditions and **TCM-15** under (b) dynamic irradiation (black, in the dark; pink, under UV-light irradiation) and (d) static irradiation (red, in the dark; gray, under UV-light irradiation) and (f) the derivative of the isotherm under dynamic conditions.

TCM-14 shows relatively low CO_2 adsorption overall, and small dynamic changes in the uptake are observed. However, under static conditions (in the dark or under continuous UV irradiation), a CO_2 uptake difference of 37% at 1 bar is observed (Figure 3). **TCM-15** performs far better than **TCM-14**, revealing a significantly larger CO_2 uptake at 293 K (CO_2 uptake of 62.3 cm^3/g at 1 bar). Under continuous UV irradiation, lower CO_2 quantities are adsorbed, whereby a static response of 29% at 1 bar is observed. Dynamic irradiation/dark cycles facilitate CO_2 desorption upon light irradiation. This leads to a desorption response of up to ca. 20% of CO_2 at 0.8−0.9 bar. The first derivatives of the dynamic switching isotherms show that the resulting inflections correspond to irradiation events and, further, that the magnitude of the photoresponse increases at higher $P(CO_2)$ pressures for both materials. This response is more pronounced for **TCM-15**, in which the incorporation of bridging azpy linkers is reduced, the framework flexibility may be greater, and potential UMCs may provide CO_2 binding sites. The extent of light-responsiveness for **TCM-15** is visualized by the derivatives of the isotherms recorded under dynamic conditions. The dynamic measurements suggest that there is no significant fatigue due to UV irradiation.

In order to rule out other effects contributing to the observed changes in uptake, control experiments were carried out using a sample containing **TCM-4** and **TCM-5**, which are nonphotoresponsive and structurally related to **TCM-14** and **TCM-15**. In control samples, no dynamic photoresponse was observed (see the SI), and the change in uptake under static irradiation was negligible.

Attenuated-total-reflectance FTIR spectroscopy was carried out at lower wavenumbers on **TCM-15** to understand the nature of structural responses corresponding to the observed change in CO_2 sorption (Figure 4). No significant intensity

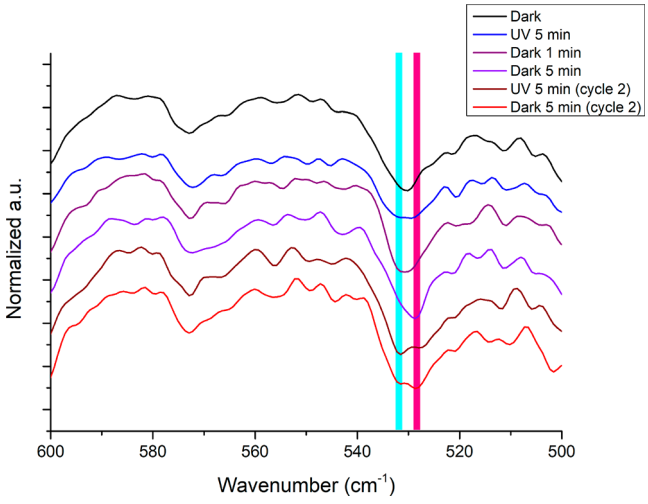

Figure 4. FTIR spectra of **TCM-15** at various stages of UV irradiation. The small shift observed between 531 and 528 cm^{-1} is highlighted using cyan and magenta bars.

increases of the vibrational bands in the 600−500 cm^{-1} window, corresponding to the C−N bending modes of azpy moieties, were observed, contrary to previous reports on the dynamic behavior in MOFs containing azobenzene-based ligands. However, upon UV irradiation, a degree of suppression of the vibrational mode at 528 cm^{-1} is apparent and is associated with a very small shift (or the emergence of a weak new signal) at 531 cm^{-1}. Therefore, despite restrictions

DOI: 10.1021/acs.inorgchem.9b00768
Inorg. Chem. XXXX, XXX, XXX−XXX

on movement of the azpy moiety, we infer that UV-irradiation-induced distortions do take place. These distortions involve changes in the bond length and are in line with suppressed cis−trans/bending isomerization mechanisms reported for the azobenzenetetracarboxylic acid (H_4abtc) ligand[21,22,25] or previously observed rotational effects.[28] Relaxation to the ground state takes place within 1 min, as confirmed by these IR studies, as well as desorption observed during the interval between the measurements of successive points on the dynamically irradiated adsorption isotherm. PXRD studies comparing powder patterns obtained for **TCM-15** before and immediately after UV irradiation show no observable difference (see the SI). The data suggest that the photoresponse is local and nonperiodic. Importantly, it confirms that simple cis−trans isomerizations of the bridging azpy ligands do not take place.

Time-dependent density functional theory (DFT) calculations were performed on a model system using *Gaussian 09* and the CAMB3LYP functional (Figure 5).[39,40] These

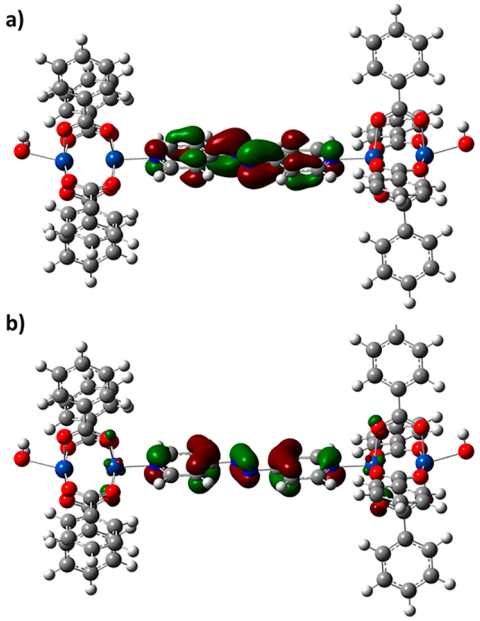

Figure 5. Time-dependent DFT-derived molecular orbital (MO) representations of a simplified $\{Cu_2\}$-azpy-$\{Cu_2\}$ model unit in **TCM-14** and **TCM-15**: (a) MO representation upon $\pi-\pi^*$ transition resulting in a localization of the MOs at the azopyridine ligand and a contribution from the binding Cu^{II} centers; (b) MO representation of the "dark" state.

calculations reveal a $\pi-\pi^*$ transition at 280 nm, in reasonable agreement with the observation given by the model system and methodology (see the SI). The orbitals involved in this transition are almost completely localized on the azopyridine ligand with a small contribution from the Cu^{II} centers directly attached to the azopyridine ligand. Such an excitation may be expected to trigger a cis−trans ligand isomerization, but this is restricted in **TCM-14** and **TCM-15** because of the constraints imposed by the 3D structure. However, the flexibility of the bteb^{3-} ligand makes the framework in **TCM-15** capable of withstanding a degree of induced distortion. One important point of difference between azpy and abtc^{4-}, and similar other azobenzene-based carboxylate linkers, is that the azpy ligands bind using monodentate N-atom donors and can rotate freely about the Cu−N bonds, subject to steric constraints. We therefore propose that the photoresponse in these materials may be due to a mechanism that facilitates small rotations or torsions about the $\{Cu_2\}$-azpy-$\{Cu_2\}$-bridged system, in addition to suppressed bending of the azpy ligand. These rotations may be occasioned by strain within the azpy ligand due to excitation and disruption of the conjugated π system and have the effect of partially obscuring the available void space. Such a mechanism is supported by the small changes observed in the IR spectra and the rapid response time observed in IR and CO_2 adsorption experiments. Indeed, similar responses due to pedal-like motion in structurally related frameworks have been reported.[28]

CONCLUSION

In summary, we report a facile synthetic methodology to functionalize **pto**-based MOFs using appropriately sized auxiliary ligands. The latter act as functionalizing templates and promote the formation of **pto**-derived topologies over other possible stereoisomeric framework structures. This approach was applied to the preparation of novel photoactive MOFs **TCM-14** and **TCM-15**. Detailed structural analyses were carried out, and we demonstrate that the CO_2 sorption characteristics are distinctively influenced by UV-light irradiation, triggering a structural response that can facilitate CO_2 desorption on demand. Significant light-induced static and dynamic responses are observed. These experimental findings are supported by spectroscopy and DFT calculations.

The presented synthetic functionalization approach is generally applicable to **pto**-type MOFs establishing a valuable synthetic proof-of-concept to rationally arrive at functional and stimuli-responsive adsorbents. Further, we anticipate advances toward the synthesis of functionalized MOFs that impact on other areas of application, e.g., sensing and catalysis, and the application of elegant synthetic and postsynthetic methods to this end.

ASSOCIATED CONTENT

Supporting Information

The Supporting Information is available free of charge on the ACS Publications website at DOI: 10.1021/acs.inorgchem.9b00768.

Ligand synthesis, experimental procedures, CHN analysis, SCXRD crystallographic data, PXRD patterns, TGA, FTIR spectra, N_2 sorption data, topological analysis, morphology images of crystals, and computational details (PDF)

Accession Codes

CCDC 1846123 and 1846124 contain the supplementary crystallographic data for this paper. These data can be obtained free of charge via www.ccdc.cam.ac.uk/data_request/cif, or by emailing data_request@ccdc.cam.ac.uk, or by contacting The Cambridge Crystallographic Data Centre, 12 Union Road, Cambridge CB2 1EZ, UK; fax: +44 1223 336033.

AUTHOR INFORMATION

Corresponding Author

*E-mail: schmittw@tcd.ie. Tel: +353-1-8963495. Fax: +353-1-6712826.

ORCID

Graeme W. Watson: 0000-0001-6732-9474

Wolfgang Schmitt: 0000-0002-0058-9404

DOI: 10.1021/acs.inorgchem.9b00768
Inorg. Chem. XXXX, XXX, XXX−XXX

Notes

The authors declare no competing financial interest.

■ ACKNOWLEDGMENTS

The authors thank Martina Schroffenegger for experimental work. Funding from the Science Foundation Ireland (SFI 13/IA/1896), the European Research Council (CoG 2014-647719), the Irish Research Council (GOIPG/2015/2952, a fellowship for S.T.), and the SFI AMBER Center is greatly acknowledged. The authors thank ICHEC for computational resources.

■ REFERENCES

(1) Goeppert, A.; Czaun, M.; Surya Prakash, G. K.; Olah, G. A. Air as the Renewable Carbon Source of the Future: An Overview of CO_2 Capture from the Atmosphere. *Energy Environ. Sci.* **2012**, *5*, 7833−7853.

(2) Huck, J. M.; Lin, L.-C.; Berger, A. H.; Shahrak, M. N.; Martin, R. L.; Bhown, A. S.; Haranczyk, M.; Reuter, K.; Smit, B. Evaluating Different Classes of Porous Materials for Carbon Capture. *Energy Environ. Sci.* **2014**, *7*, 4132−4146.

(3) Furukawa, H.; Cordova, K. E.; O'Keeffe, M.; Yaghi, O. M. The Chemistry and Applications of Metal−Organic Frameworks. *Science* **2013**, *341*, 1230444.

(4) Yan, Q.; Zhou, R.; Fu, C.; Zhang, H.; Yin, Y.; Yuan, J. CO_2-responsive polymeric vesicles that breathe. *Angew. Chem., Int. Ed.* **2011**, *50*, 4923−4927.

(5) Coudert, F. X. Responsive Metal−Organic Frameworks and Framework Materials: Under Pressure, Taking the Heat, in the Spotlight, with Friends. *Chem. Mater.* **2015**, *27*, 1905−1916.

(6) Jones, C. L.; Tansell, A. J.; Easun, T. L. The Lighter Side of MOFs: Structurally Photoresponsive Metal−Organic Frameworks. *J. Mater. Chem. A* **2016**, *4*, 6714−6723.

(7) Li, H.; Hill, M. R. Low-Energy CO_2 Release from Metal−Organic Frameworks Triggered by External Stimuli. *Acc. Chem. Res.* **2017**, *50*, 778−786.

(8) Li, H.; Davis, C. E.; Groy, T. L.; Kelley, D. G.; Yaghi, O. M. Coordinatively Unsaturated Metal Centers in the Extended Porous Framework of $Zn_3(BDC)_3{\cdot}6CH_3OH$ (BDC = 1,4-benzenedicarboxylate). *J. Am. Chem. Soc.* **1998**, *120*, 2186−2187.

(9) Zhu, N.; Lennox, M. J.; Düren, T.; Schmitt, W. Polymorphism of Metal−organic Frameworks: Direct Comparison of Structures and Theoretical N_2-Uptake of Topological **pto**- and **tbo**-Isomers. *Chem. Commun.* **2014**, *50*, 4207−4210.

(10) Zhu, N.; Lennox, M. J.; Tobin, G.; Goodman, L.; Düren, T.; Schmitt, W. Hetero-Epitaxial Approach by Using Labile Coordination Sites to Prepare Catenated Metal−Organic Frameworks with High Surface Areas. *Chem. - Eur. J.* **2014**, *20*, 3595−3599.

(11) Klein, N.; Senkovska, I.; Baburin, I. A.; Grünker, R.; Stoeck, U.; Schlichtenmayer, M.; Streppel, B.; Mueller, U.; Leoni, S.; Hirscher, M.; Kaskel, S. Route to a Family of Robust, Non-Interpenetrated Metal−Organic Frameworks with **pto**-like Topology. *Chem. - Eur. J.* **2011**, *17*, 13007−13016.

(12) Müller, P.; Grünker, R.; Bon, V.; Pfeffermann, M.; Senkovska, I.; Weiss, M. S.; Feng, X.; Kaskel, S. Topological Control of 3,4-Connected Frameworks Based on the Cu_2-Paddle-Wheel Node: **tbo** or **pto**, and Why? *CrystEngComm* **2016**, *18*, 8164−8171.

(13) Horike, S.; Shimomura, S.; Kitagawa, S. Soft Porous Crystals. *Nat. Chem.* **2009**, *1*, 695−704.

(14) Yanai, N.; Uemura, T.; Inoue, M.; Matsuda, R.; Fukushima, T.; Tsujimoto, M.; Isoda, S.; Kitagawa, S. Guest-to-Host Transmission of Structural Changes for Stimuli- Responsive Adsorption Property. *J. Am. Chem. Soc.* **2012**, *134*, 4501−4504.

(15) Lyndon, R.; Konstas, K.; Evans, R. A.; Keddie, D. J.; Hill, M. R.; Ladewig, B. P. Tunable Photodynamic Switching of DArE@PAF-1 for Carbon Capture. *Adv. Funct. Mater.* **2015**, *25*, 4405−4411.

(16) Li, H.; Hill, M. R.; Doblin, C.; Lim, S.; Hill, A. J.; Falcaro, P. Visible Light Triggered CO_2 Liberation from Silver Nanocrystals Incorporated Metal−Organic Frameworks. *Adv. Funct. Mater.* **2016**, *26*, 4815−4821.

(17) Modrow, A.; Zargarani, D.; Herges, R.; Stock, N. The First Porous MOF with Photoswitchable Linker Molecules. *Dalton Trans.* **2011**, *40*, 4217−4222.

(18) Modrow, A.; Zargarani, D.; Herges, R.; Stock, N. Introducing a Photo-Switchable Azo-Functionality inside Cr-MIL-101-NH_2 by Covalent Post-Synthetic Modification. *Dalton Trans.* **2012**, *41*, 8690−8696.

(19) Bernt, S.; Feyand, M.; Modrow, A.; Wack, J.; Senker, J.; Stock, N. A Mixed-Linker ZIF Containing a Photoswitchable Phenylazo Group. *Eur. J. Inorg. Chem.* **2011**, *2011*, 5378−5383.

(20) Brown, J. W.; Henderson, B. L.; Kiesz, M. D.; Whalley, A. C.; Morris, W.; Grunder, S.; Deng, H.; Furukawa, H.; Zink, J. I.; Stoddart, J. F.; Yaghi, O. M. Photophysical Pore Control in an Azobenzene-containing Metal−organic Framework. *Chem. Sci.* **2013**, *4*, 2858−2864.

(21) Park, J.; Yuan, D.; Pham, K. T.; Li, J. R.; Yakovenko, A.; Zhou, H. C. Reversible Alteration of CO_2 Adsorption upon Photochemical or Thermal Treatment in a Metal−Organic Framework. *J. Am. Chem. Soc.* **2012**, *134*, 99−102.

(22) Lyndon, R.; Konstas, K.; Ladewig, B. P.; Southon, P. D.; Kepert, P. C. J.; Hill, M. R. Dynamic Photo-Switching in Metal−Organic Frameworks as a Route to Low-Energy Carbon Dioxide Capture and Release. *Angew. Chem., Int. Ed.* **2013**, *52*, 3695−3698.

(23) Luo, F.; Fan, C. B.; Luo, M. B.; Wu, X. L.; Zhu, Y.; Pu, S. Z.; Xu, W.-Y.; Guo, G.-C. Photoswitching CO_2 Capture and Release in a Photochromic Diarylethene Metal−Organic Framework. *Angew. Chem., Int. Ed.* **2014**, *53*, 9298−9301.

(24) Gong, L. L.; Feng, X. F.; Luo, F. Novel Azo-Metal−Organic Framework Showing a 10-Connected **bct** Net, Breathing Behavior, and Unique Photoswitching Behavior toward CO_2. *Inorg. Chem.* **2015**, *54*, 11587−11589.

(25) Li, H.; Martinez, M. R.; Perry, Z.; Zhou, H.-C.; Falcaro, P.; Doblin, C.; Lim, S.; Hill, A. J.; Halstead, B.; Hill, M. R. A Robust Metal−Organic Framework for Dynamic Light-Induced Swing Adsorption of Carbon Dioxide. *Chem. - Eur. J.* **2016**, *22*, 11176−11179.

(26) Jiang, Y.; Tan, P.; Qi, S.-C.; Liu, X.-Q.; Yan, J.-H.; Fan, F.; Sun, L.-B. Metal−Organic Frameworks with Target-Specific Active Sites Switched by Photoresponsive Motifs: Efficient Adsorbents for Tailorable CO_2 Capture. *Angew. Chem., Int. Ed.* **2019**, *58*, 6600−6604.

(27) Cheng, L.; Jiang, Y.; Qi, S.; Liu, W.; Shan, S.; Tan, P.; Liu, X.; Sun, L. Controllable Adsorption of CO_2 on Smart Adsorbents: An Interplay between Amines and Photoresponsive Molecules. *Chem. Mater.* **2018**, *30*, 3429−3437.

(28) Song, W. C.; Cui, X. Z.; Liu, Z. Y.; Yang, E. C.; Zhao, X. J. Light-Triggered Supramolecular Isomerism in a Self-Catenated Zn(II)−Organic Framework: Dynamic Photo-Switching CO_2 Uptake and Detection of Nitroaromatics. *Sci. Rep.* **2016**, *6*, 1−8.

(29) Takeuchi, M.; Ikeda, M.; Sugasaki, A.; Shinkai, S. Molecular Design of Artificial Molecular and Ion Recognition Systems with Allosteric Guest Responses. *Acc. Chem. Res.* **2001**, *34*, 865−873.

(30) Browne, W. R.; Feringa, B. L. Making Molecular Machines Work. *Nat. Nanotechnol.* **2006**, *1*, 25−35.

(31) Irie, M. Diarylethenes for Memories and Switches. *Chem. Rev.* **2000**, *100*, 1685−1716.

(32) Zhu, N.; Tobin, G.; Schmitt, W. Extending the Family of Zn-Based MOFs: Synthetic Approaches to Chiral Framework Structures and MOFs with Large Pores and Channels. *Chem. Commun.* **2012**, *48*, 3638−3640.

(33) Zhu, N.; Sensharma, D.; Wix, P.; Lennox, M. J.; Düren, T.; Wong, W.-Y.; Schmitt, W. Framework Isomerism: Highly Augmented Copper(II)-Paddlewheel-Based MOF with Unusual (3,4)-Net Topology. *Eur. J. Inorg. Chem.* **2016**, *2016*, 1939−1943.

(34) Furukawa, H.; Ko, N.; Go, Y. B.; Aratani, N.; Choi, S. B.; Choi, E.; Yazaydin, A. O.; Snurr, R. Q.; O'Keeffe, M.; Kim, J.; Yaghi, O. M. Ultrahigh Porosity in Metal−Organic Frameworks. *Science* **2010**, *329*, 424−428.

DOI: 10.1021/acs.inorgchem.9b00768
Inorg. Chem. XXXX, XXX, XXX−XXX

(35) Castellano, R. K.; Rebek, J. Formation of Discrete, Functional Assemblies and Informational Polymers through the Hydrogen-Bonding Preferences of Calixarene Aryl and Sulfonyl Tetraureas. *J. Am. Chem. Soc.* **1998**, *120*, 3657−3663.
(36) Blatov, V. A.; Shevchenko, A. P.; Proserpio, D. M. Applied Topological Analysis of Crystal Structures with the Program Package ToposPro. *Cryst. Growth Des.* **2014**, *14*, 3576−3586.
(37) Liu, L.; Konstas, K.; Hill, M. R.; Telfer, S. G. Programmed Pore Architectures in Modular Quaternary Metal−Organic Frameworks. *J. Am. Chem. Soc.* **2013**, *135*, 17731−17734.
(38) Hönicke, I. M.; Senkovska, I.; Bon, V.; Baburin, I. A.; Bönisch, N.; Raschke, S.; Evans, J. D.; Kaskel, S. Balancing Mechanical Stability and Ultrahigh Porosity in Crystalline Framework Materials. *Angew. Chem., Int. Ed.* **2018**, *57*, 13780−13783.
(39) Frisch, M. J.; Trucks, G. W.; Schlegel, H. B.; Scuseria, G. E.; Robb, M. A.; Cheeseman, J. R.; Scalmani, G.; Barone, V.; Mennucci, B.; Petersson, G. A.; Nakatsuji, H.; Caricato, M.; Li, X.; Hratchian, H. P.; Izmaylov, A. F.; Bloino, J.; Zheng, G.; Sonnenberg, J. L.; Hada, M.; Ehara, M.; Toyota, K.; Fukuda, R.; Hasegawa, J.; Ishida, M.; Nakajima, T.; Honda, Y.; Kitao, O.; Nakai, H.; Vreven, T.; Montgomery, J. A., Jr.; Peralta, J. E.; Ogliaro, F.; Bearpark, M.; Heyd, J. J.; Brothers, E.; Kudin, K. N.; Staroverov, V. N.; Kobayashi, R.; Normand, J.; Raghavachari, K.; Rendell, A.; Burant, J. C.; Iyengar, S. S.; Tomasi, J.; Cossi, M.; Rega, N.; Millam, N. J.; Klene, M.; Knox, J. E.; Cross, J. B.; Bakken, V.; Adamo, C.; Jaramillo, J.; Gomperts, R.; Stratmann, R. E.; Yazyev, O.; Austin, A. J.; Cammi, R.; Pomelli, C.; Ochterski, J. W.; Martin, R. L.; Morokuma, K.; Zakrzewski, V. G.; Voth, G. A.; Salvador, P.; Dannenberg, J. J.; Dapprich, S.; Daniels, A. D.; Farkas, O.; Foresman, J. B.; Ortiz, J. V.; Cioslowski, J.; Fox, D. J. *Gaussian 09*, revision A.02; Gaussian Inc.: Wallingford, CT, 2009.
(40) Yanai, T.; Tew, D. P.; Handy, N. C. A New Hybrid Exchange-Correlation Functional Using the Coulomb-Attenuating Method (CAM-B3LYP). *Chem. Phys. Lett.* **2004**, *393*, 51−57.

DOI: 10.1021/acs.inorgchem.9b00768
Inorg. Chem. XXXX, XXX, XXX−XXX